



# The effect of ice rheology on shelf edge bending

W. Roger Buck

Lamont-Doherty Earth Observatory of Columbia University, 61 Rt. 9w Palisades, NY 10960, USA

*Correspondence to:* W. Roger Buck (buck@ldeo.columbia.edu)

5 **Abstract.** The distribution of water pressure on the vertical front of an ice shelf has been shown to cause downward bending  
of the edge if the ice has vertically uniform viscosity. Satellite lidar observations show upward bending of shelf edges for some  
areas with cold surface temperatures. A simple analysis shows that upward bending of shelf edges can result from vertical  
variations in ice viscosity. Such variations are an expected consequence of the temperature dependence of ice viscosity and  
temperature variations through a shelf. Resultant vertical variations in horizontal stress produce an internal bending moment  
10 that can counter the bending moment due to the shelf-front water pressure. Assuming a linear profile of ice temperature with  
depth and an Arrhenius relation between temperature and strain rate allows derivation of an analytic expression for internal  
bending moments. The effect of a power-law relation between stress difference and strain rate is also included analytically.  
The key ice rheologic parameter affecting shelf edge bending is the ratio of the activation energy,  $Q$ , and the power-law  
exponent,  $n$ . For cold ice surface temperatures and large values of  $Q/n$ , upward bending is expected, while for warm surface  
15 temperatures and small values of  $Q/n$  downward bending is expected. The amplitude of bending should scale with the ice shelf  
thickness to the power  $3/2$  and this is approximately consistent with a recent analysis of shelf edge deflections for the Ross Ice  
Shelf.

## 1 Introduction

Ice shelf bending may lead to calving and break up of shelves in two ways. Bending stresses may lead directly to crevasse  
20 formation and propagation (e.g. Wagner et al., 2016). Bending may also affect the routing and pooling of surface meltwater,  
which can facilitate crevasse growth and calving (e.g. Weertman, 1973; Lai et al., 2020; Buck, 2023). Ice shelf breakup is of  
concern since it could reduce the buttressing of ice sheets, leading to a speed up of ice sheet flow and therefor a rise of sea  
level (Scambos et al., 2004; Rignot et al., 2004; Schoof, 2007; Gudmundsson, 2013; Fürst et al., 2016). Long-term models of  
ice sheet flow predict accelerated sea-level rise caused by loss of ice shelves (e.g. DeConto et al., 2021).

25

The rheology of ice is critical to ice shelf calving and to flow of ice sheets and shelves (e.g. Cuffey and Patterson, 2010).  
Laboratory and theoretical analyses suggest that ice flow can be described as a non-Newtonian viscous fluid (Glen, 1955) with  
a strong temperature dependence (e.g. Weertman, 1983). However, there is great uncertainty in the parameters that describe



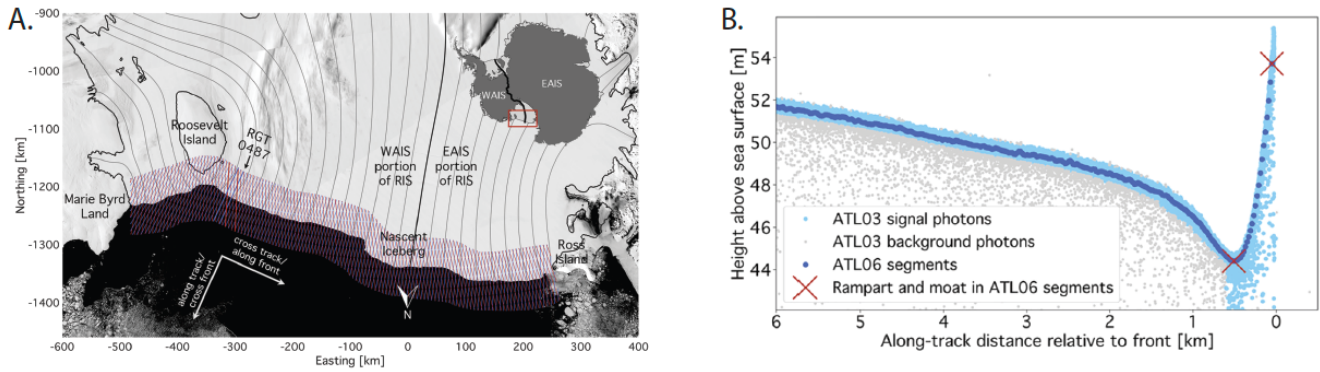
ice flow (e.g. Cuffey and Patterson, 2010; Behn et al., 2021, Zeitz et al., 2020; Millstein, et al., 2022). Analysis of ice shelf  
30 bending may provide an additional constraint on ice rheology.

The downward bending of ice shelf edges is expected to result from the bending moment due to the pressure in water exerted  
on the shelf. Weertman (1957) derived an expression for this bending moment as a function of ice and water densities,  
assuming a uniform ice rheology with depth. Reeh (1968) numerically calculated the deflections due to this bending moment  
35 by treating the ice shelf as a uniform thin viscous plate and showed how the downward deflections of the edge would increase  
with time since the last calving event, as viscous stresses relax. Fully two-dimensional viscous (Mosbeux et al, 2021) and  
visco-elastic models (Christmann et al, 2019) of ice shelf bending, assuming uniform properties with depth, confirm the thin-  
plate predictions.

40 The down-bending of shelf edges predicted by the Weertman-Reeh theory has been seen in several locations, but the opposite  
sense of bending has been observed in several other areas (e.g. Scambos et al, 2005, 2008, Becker et al., 2021). That many  
shelf edges bend upward with a high “rampart” at the shelf edge paired with a pronounced low “moat” inward of the edge and  
has generated great interest (e.g. Wagner et al., 2014, 2016; Mosbeux et al, 2021). For example, a comprehensive study of the  
Ross Ice Shelf by Becker et al (2021) using ICESat 2 lidar shows that moats and ramparts are separated by horizontal offsets  
45 of a few hundred meters with typical elevation differences of 5 to 10 meters (Fig. 1).

The only published model for rampart-moat structures relates to erosion of part of the sub-aerial shelf by wave action (Scambos  
et al., 2005; Wagner et al., 2016; Mosbeux et al., 2020, Becker et al., 2021). The submarine remnant, termed a “foot” or  
“bench,” then acts as a load that pushes up the un-eroded shelf edge (Fig. 2). Bench-driven up-bending can increase the  
50 magnitude of extensional stresses under the moat that could drive basal crevassing and calving (Wagner et al., 2014; 2016).

This study considers an alternative model to the submerged bench model that depends on vertical variations in the viscosity of  
an ice shelf. In some sense this work is a continuation of the analysis of Reeh (1968) in that it deals with bending moments  
causing an ice shelf to flex. In the pioneering paper on that topic, Reeh (1968) wrote: “... a correct treatment of the problem  
55 would require consideration of the great variation (by a factor ten or more) of the viscosity. This, however, would involve  
enormous mathematical troubles.” Here I show that, as long as we can assume that the viscosity in an ice shelf varies  
exponentially with depth, the “mathematical troubles” are minimal. Below I show that the exponential viscosity approximation  
is reasonable if the temperature dependence of viscosity can be described by an Arrhenius relation and the temperatures  
increase linearly with depth in an ice shelf. That approximation allows derivation of scaling relations between ice rheologic  
60 parameters, ice surface temperatures and shelf edge deflections. For “great variations of viscosity” across an ice shelf I show  
that the edge of the shelf should bend upward to make a rampart with a corresponding inboard moat. Before launching into a  
detailed analysis of this problem I discuss some basic ideas about bending moments and layer bending.



65 **Figure 1: Example topographic relief of the Ross Ice Shelf edge. (A) IceSat-2 track lines, and (B) topography showing characteristic “moat and rampart” relief. (both from Becker et al. 2021).**

## 2 Conceptual model

Ice shelves that are not heavily buttressed are under extension (Weertman, 1957) and vertical variations in viscosity imply vertical gradients in horizontal stress. The idea that stresses internal to a layer can cause it to bend is well known in engineering and can be illustrated with a bi-metallic strip that bends as temperatures change. Such a strip consists of two metal layers with different thermal expansion coefficients that are welded together. At a certain temperature this layered strip can be flat, but it will “curl up” when the temperature is increased as long as the lower layer has a larger thermal expansion coefficient. This occurs because the lower layer expands more than the upper layer producing vertical variations in horizontal stress.

75 Parmentier and Haxby (1986) showed how vertical variations of horizontal stress within a strong layer might explain downward bending of lithosphere at transform faults. Those authors note that gravity prevents lithospheric bending that is of much longer wavelength than the effective flexural wavelength of the layer. At very long length scales gravity prevents the layer from bending. The vertical variation in stress can be thought of as an internal bending moment that is everywhere matched by adjacent bending moments except at the plate edge (transform fault) where stresses, and so the applied bending moment, are different.

The concept of internal bending moments was applied to the formation of “axial highs” that mark the plate boundary at most fast-spreading centers and typically rise 300-500 meters above the surrounding seafloor (Buck, 2001). That paper showed that the deflection of a plate with a free end and a uniform internal moment are equivalent to that resulting from application of an opposite moment to the end of a layer with no internal moment.

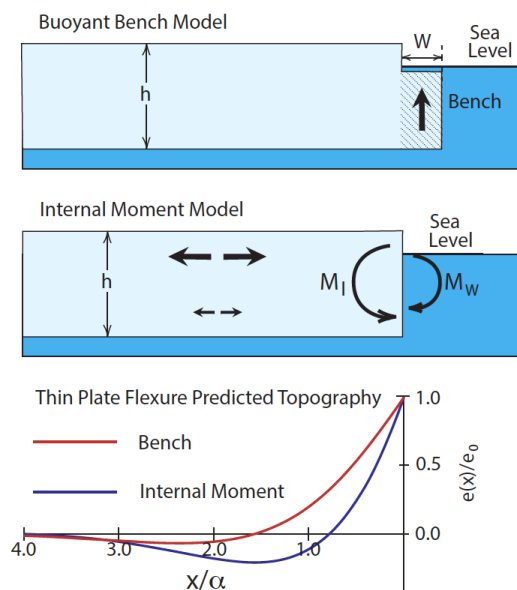
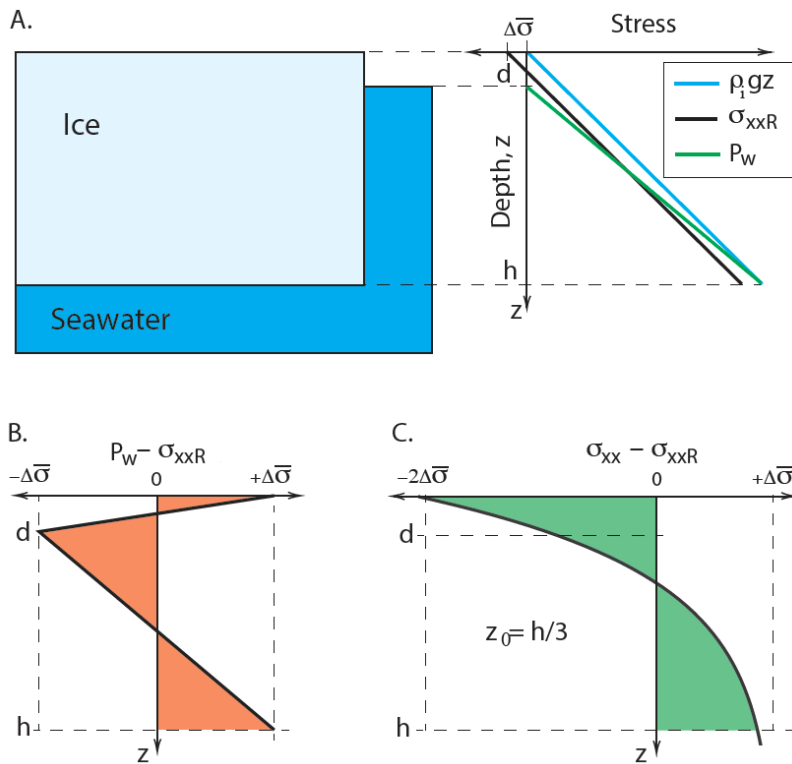


**Figure 2: Illustrations of the bench and internal moment models for deflection of a shelf edge. The arrow on the top sketch indicates the upward force due to a submerged ice “bench.” The internal moment arises from vertical variations in horizontal stress (indicated by horizontal arrows on the internal moment sketch).  $M_w$  and  $M_i$  are the applied moments due the pressure distribution of water and the internal stress variations, respectively. The plot at the bottom shows the thin plate model predictions of the model vertical deflections  $e$  as a function of distance from a shelf edge for equations 1 and 2, where  $e_0$  is the deflection at the shelf edge (see text for explanation).**

90 As noted by Reeh (1968) the top of an ice shelf is typically colder than the base (by as much as 30°C) and so viscosity decreases with depth in the shelf. There is a corresponding decrease in extensional stress with depth and this implies that there is an internal bending moment in the shelf. Where the shelf is laterally uniform and continuous over distances much larger than the flexural wavelength, the shelf should be flat. Imagine that a calving event just broke off a broad section of the shelf making a new shelf edge. If the bending moment applied by air and water at the shelf edge is different from the internal bending moment  
 100 then the shelf edge should bend, much like the bi-metallic strip described above.

In the absence of a bench, it is the internal stress distribution that determines whether the edge bends up or down. The key question for this paper is how the horizontal stresses internal to an ice shelf affect the bending of a shelf edge. To do this I follow the approach of Weertman (1957) and Reeh (1968) and calculate the contribution to the total applied bending moment  
 105 due to the difference between water pressure and internal stress in the ice layer. The new twist is that I consider internal stress variations related to vertical viscosity variations in the ice shelf.



110 **Figure 3: Illustrations of stresses and stress differences affecting a floating ice layer. (a) shows an ice layer of thickness**  
**h floating on seawater with a surface at a depth  $d$  below the top of the ice. The green line shows pressures in seawater**  
**and the blue shows the vertical stress in the ice. The black line shows the reference horizontal stress  $\sigma_{xxR}$  in the ice**  
**which is offset by a constant stress difference  $\Delta \bar{\sigma}$  from the vertical stress. (b) shows the difference between the water**  
**pressure and the reference horizontal stress. (c) shows the difference between an example exponentially varying**  
 115 **horizontal stress in the ice (with  $z_0 = h/3$ ) and the reference horizontal stress. Note that the average of the stress**  
**differences in B and C are zero. The first moment of those stress differences with depth equals the “water moment” (in**  
**b) and the “internal moment” (in c) as defined in the text.**

### 3. Analytic Model

#### 3.1 Stresses, Pressures and Bending Moments

120 To determine how an ice layer will flex due to the water pressure distribution on the side of the layer (as shown in Fig. 3) we  
 need to calculate the total applied bending moment  $M_T$  due to the difference between pressure of the water and the horizontal  
 stress in the ice:



$$M_T = - \int_0^h [P_w(z) - \sigma_{xx}(z)]zdz \quad (1)$$

125 where the arbitrary minus sign ensures that upward bending corresponds to positive total applied moments. The pressure in the water that acts on the side of the floating ice layer is:

$$P_w(z) = \begin{cases} 0 & \text{for } z < d \\ \rho_w g(z - d) & \text{for } h > z > d \end{cases} \quad (2)$$

130 where  $\rho_w$  is the density of water,  $h$  is the thickness of the ice layer,  $z$  is depth below the ice surface  $g$  is the acceleration of gravity and  $d$  is the freeboard height shown on Fig. 2. Equating the vertical stress and water pressure at  $z = h$  requires that:

$$d = \left( \frac{\rho_w - \rho_i}{\rho_w} \right) h \quad (3)$$

assuming that the vertical stress,  $\sigma_{zz}$ , in the ice is:

$$\sigma_{zz}(z) = \rho_i g z \quad (4)$$

135 where  $\rho_i$  is the density of ice. I use the geologic convention that positive stress is compressive to simplify the comparison of water pressures and ice stresses.

A horizontal force balance requires that:

$$F_x = \int_0^h \sigma_{xx}(z)dz = \int_d^h P_w(z)dz \quad (5)$$

140 where  $\sigma_{xx}(z)$  is the horizontal stress in the layer.

To consider the effect on layer edge bending for a range of possible distributions of the horizontal stress that satisfy equation (5) it is useful to define a reference horizontal stress distribution  $\sigma_{xxR}(z)$ . This allow separate calculation of the applied moments due to the water pressures,  $M_W$ , and the horizontal stresses with the ice,  $M_I$ , relative to that reference, such that equation (1) can be re-written:

$$145 \quad M_T = M_W + M_I = - \int_0^h [P_w(z) - \sigma_{xxR}(z)]zdz + \int_0^h [\sigma_{xx}(z) - \sigma_{xxR}(z)]zdz. \quad (6)$$

The reference horizontal stress distribution is what would obtain for a shelf with uniform rheologic properties, so that the horizontal stress is lower than the vertical stress by a uniform amount,  $\Delta\bar{\sigma}$ . As noted by Weertman (1957), the value of the average stress difference  $\Delta\bar{\sigma}$  at the edge of an ice shelf (or within a shelf where buttressing forces are zero) is constrained by equations (5) and (2) and can be written:

$$150 \quad \Delta\bar{\sigma} = \sigma_{zz}(z) - \frac{F_x}{h} = \frac{1}{2} \left( \frac{\rho_i}{\rho_w} \right) (\rho_w - \rho_i) gh. \quad (7)$$



so that:

$$\sigma_{xxR}(z) \equiv \sigma_{zz}(z) - \Delta\bar{\sigma} = \rho_i g z - \frac{1}{2} \left( \frac{\rho_i}{\rho_w} \right) (\rho_w - \rho_i) g h \quad (8)$$

For  $\Delta\bar{\sigma}$  given by equation (7) the bending moment term related to the water pressure variation is:

$$M_W = - \int_0^h [P_w(z) - \sigma_{xxR}(z)] z dz = - \frac{1}{12} \left( \frac{\rho_i}{\rho_w} \right) (\rho_w - \rho_i) g h^3 \left[ 1 - \frac{2d}{h} \right], \quad (9)$$

155 which is equivalent to that found by Weertman (1957) and Reeh (1968). The internal bending moment term  $M_I$  is:

$$M_I = \int_0^h [\sigma_{xx}(z) - \sigma_{xxR}(z)] z dz \quad (10)$$

and below I consider cases for different distributions of the horizontal stress with depth in the ice.

The simplest case is for an ice layer with vertically uniform properties and infinite yield strength (or infinite fracture  
160 toughness) so there is no opening of surface or basal crevasses thus reducing the stresses in the layer. This implies a  
constant offset between the horizontal and vertical stresses in the layer such that  $\sigma_{xx}(z) = \sigma_{xxR}(z)$  implying that  $M_I = 0$  so  
that  $M_T = M_W$ . In this case the moment applied to the end of the layer bends it down. Assuming  $\rho_i/\rho_w = 0.9$  in equation (3)  
means that  $d = h/10$  so that  $M_T = M_W = \left( \frac{1}{15} \right) \left( \frac{\rho_i}{\rho_w} \right) (\rho_w - \rho_i) g h^3$ .

165 Reeh (1968) calculated that the the applied bending moment increases by up to 30% as the layer is deflected, because as the  
shelf edge moves down the water pressure on the end increases. However, this neglects the counter effect of the change in  
pressure on the underside of the deflected layer inboard of the edge. Thus, the average horizontal stress in the ice should remain  
constant as long as the thickness of the shelf does not change or the top of the layer does not drop below the water surface.  
Here, I neglect any changes in the applied moment with layer deflection.

### 170 3.2 Exponential Variation of Effective Viscosity with Depth

As noted above viscosity in an ice shelf is expected to decrease with depth (e.g. Reeh, 1968). Two simplifying assumptions  
are used here to relate viscosity variations with depth to rheologic parameters and ice shelf surface temperatures. The first  
assumption is that temperatures linearly increase with depth. The base of ice shelf should be at the pressure melting point while  
the surface must be colder (e.g. Cuffey and Patterson, 2010) and borehole measurements on some ice shelves indicate nearly  
175 linear temperature-depth profiles (e.g. MacAyeal and Thomas, 1979). Thus, effects of such as surface or basal melting or  
accumulation that can cause significant departures from uniform temperature gradients are ignored in this study.



180 The second assumption is the form of the ice flow law. There is debate about how the flow of ice varies with stress and temperature and there is evidence that multiple processes require complex descriptions (e.g. Behn et al, 2021). However, a wide range of observations and laboratory data are well approximated with a power-law relation between stress and strain rate, such as Glen’s flow law (Glen, 1955), and an Arrhenius relation between strain rate and temperature (e.g. Cuffey and Patterson, 2010). Then the strain rate  $\dot{\epsilon}$  is related to stress difference  $\Delta\sigma$  and absolute temperature  $T$  as:

$$\dot{\epsilon} = A\Delta\sigma^n \exp\left(\frac{-Q}{RT}\right) \quad (11)$$

185 where  $A$  and  $n$  are constants,  $Q$  is the activation energy and  $R$  is the universal gas constant. The effective viscosity  $\eta$  ( $=\Delta\sigma/\dot{\epsilon}$ ) at a constant strain rate is then:

$$\eta(\dot{\epsilon}, T) = A^{-1/n} \dot{\epsilon}^{\left(\frac{1}{n}-1\right)} \exp\left(\frac{Q}{nRT}\right). \quad (12)$$

A constant strain rate is used because the horizontal strain rate should be constant with depth for a uniform thickness ice shelf far from the shelf edge (i.e. where  $x \gg h$  and  $x$  is distance from the edge).

190 For a constant temperature gradient  $dT/dz$  we can describe the temperature with depth in the ice as:

$$T = T_s + \frac{dT}{dz} z = T_s + \frac{(T_B - T_s)}{h} z \quad (13)$$

where  $T_s$  is the temperature at the surface and  $T_B$  is the temperature at the base of the ice shelf as shown in Fig. 4. Assuming that  $Q/n$  is constant with temperature and that temperature variations in the ice are small compared to the absolute surface temperature, allowing use of the binomial theorem to approximate equation (12) as:

195  $\eta(\dot{\epsilon}, z) \cong \eta(\dot{\epsilon}, T_s) \exp\left(\frac{-z}{z_0}\right)$  (14)

where the “e-folding” length for viscosity variations is:

$$z_0 = \frac{nRT_s^2}{Q \frac{dT}{dz}} \quad \text{or} \quad \frac{z_0}{h} = \frac{nRT_s^2}{Q(T_B - T_s)} \quad (15)$$

Figure 4 confirms that, with a linear temperature profile through an ice shelf, equation (14) is an excellent approximation to the Glen’s flow law relation given by equation (12) for reasonable rheologic parameters and surface temperatures.

200



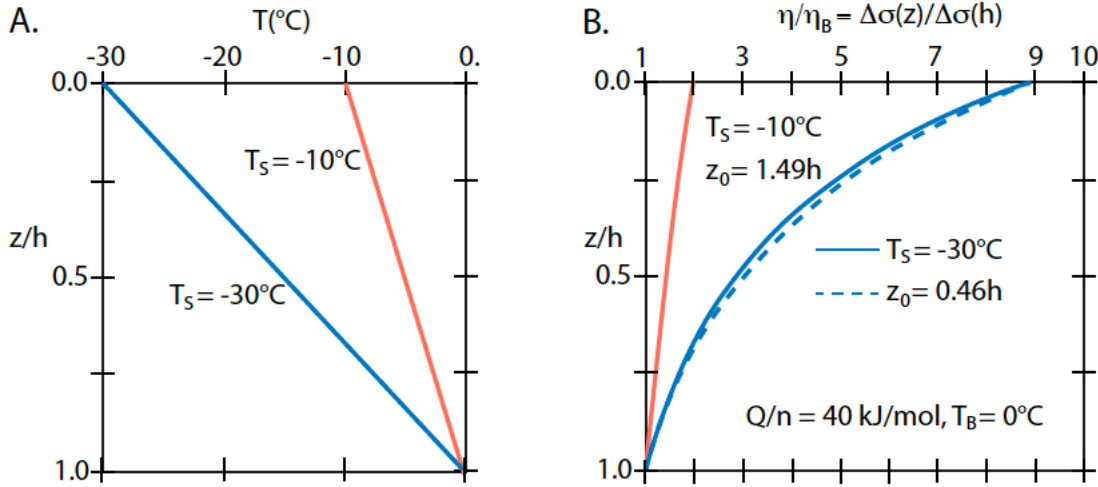


**Figure 4: (a) Relations between temperatures with depth divided by the ice layer thickness in the ice shelf and (b) the ratio of effective viscosity (or stress difference) at a constant strain rate to the viscosity (or stress difference) at the base of the layer based on the standard Glen-type flow law (equation (12)) as a solid line and the exponential approximation (equation (14)) as a dashed line. For this example the activation energy  $Q$  divided by the power-law exponent  $n$  is 40 kJ/mol. For a surface temperature  $T_s = -10^\circ\text{C}$  there is no visible difference in the two values of viscosity or stress difference and for  $T_s = -30^\circ\text{C}$  the difference is minor.**

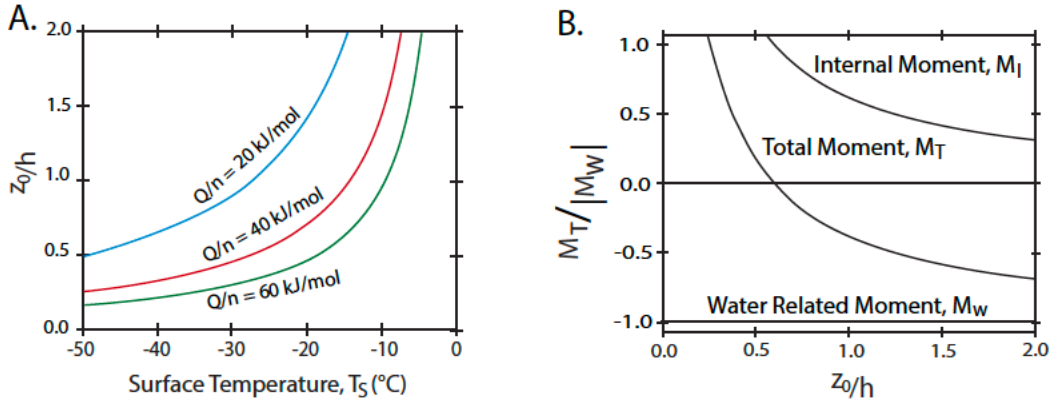
For a thin floating layer, the horizontal strain rate far from the sides (i.e. many layer thicknesses) should be constant so that the difference between the horizontal stress and the vertical stress is well approximated as:

$$\Delta\sigma(z) = \sigma_{zz}(z) - \sigma_{xx}(z) = \eta(\dot{\epsilon}, z) \dot{\epsilon} \cong \Delta\sigma_0 \exp\left(\frac{-z}{z_0}\right) \quad (16)$$

where the stress difference at the surface is:

$$\Delta\sigma_0 = \eta(\dot{\epsilon}, T_s) \dot{\epsilon} = \left(\frac{\dot{\epsilon}}{A}\right)^{\frac{1}{n}} \exp\left(\frac{Q}{nRT_s}\right). \quad (17)$$

The relationship between  $z_0/h$  and  $T_s$  is shown in Fig. 5 for a range of values of  $Q/n$  assuming for simplicity that  $T_B = 0^\circ\text{C}$ .



220 **Figure 5: (a) Relations between the non-dimensional e-folding depth scale  $z_0/h$  and the surface temperature assuming Glen's flow law (equation 11 with the rheologic parameters indicated) and that the base of the shelf is at a temperature of 0°C for the approximation described in the text and given in equation 14. (b) Shows relations between and the components of the moments as functions of  $z_0/h$ .**

We do not need to know the strain rate to find  $\sigma_0$  since it set by the force applied by water at the front of the ice shelf given by equations (2) and (5). Integration of equation (16) over the depth range of the ice shelf implies that:

$$\Delta\sigma_0 = \Delta\bar{\sigma} \left(\frac{h}{z_0}\right) \left[1 - \exp\left(\frac{-h}{z_0}\right)\right]^{-1} \quad (18)$$

230 Figure 4 shows how the horizontal stress difference varies relative to the stress at the layer base for values of  $z_0/h$  defined for given values of  $Q/n$  and for 2 values of the surface temperature. For surface temperature warmer than -10 °C the horizontal stresses at all depths are nearly equal to the basal stress and that implies a nearly constant offset between the horizontal and vertical stresses. For colder surface temperatures the horizontal stress differences near the surface are far more extensional than deeper in the layer.

The internal bending moment given by equation (10) for the stress distribution of equation (18) is:

$$M_I = \frac{1}{2} \left(\frac{\rho_i}{\rho_w}\right) (\rho_w - \rho_i) g h^3 \left\{ \left[ \frac{z_0}{h} - \left(\frac{z_0}{h} + 1\right) \exp\left(\frac{-h}{z_0}\right) \right] \left[ 1 - \exp\left(\frac{-h}{z_0}\right) \right]^{-1} - \frac{1}{2} \right\} \quad (19)$$

235 Equation (19) implies that the internal bending moment and so the bending of a layer depends on the ice and seawater densities, the layer thickness,  $h$ , and the e-folding depth,  $z_0$ , for viscosity variations. Figure 5 shows the relation between the internal moment and  $z_0/h$ . For  $z_0 \gg h$  the internal moment is zero which makes sense because the horizontal stresses are equal to the reference stresses at all depths. For  $z_0 \ll h$  the maximum value of  $M_I$  is  $-0.5 \Delta\bar{\sigma}_{max} h^2$ . We find that if  $z_0/h \approx 0.6$  that the



internal moment is equal and opposite in sign to the moment applied by the water. This would give no bending of the layer.  
 240 For a larger values of  $z_0$  the layer bends down and for a smaller values the layer bends up! Figure 6 shows how the surface temperature affects the total bending moment for different values of the rheologic parameter  $Q/n$ .

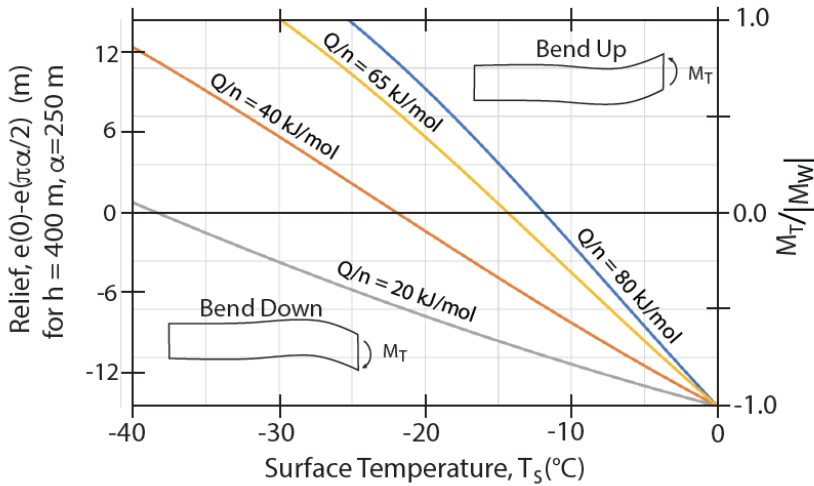


**Figure 6: Analytic model predictions of the total bending moment versus surface temperature for the indicated values of the rheologic parameter  $Q/n$ .** The vertical scale on the right shows the total moment divided by the absolute value of the moment of water pressure for a uniform rheology ice shelf. The scale on the left is the predicted height difference between the shelf edge and the closest position with zero slope (i.e. where the surface is horizontal) for a thin plate with the indicated ice thickness and flexural parameter.

### 3.3 Topographic variation based on the thin plate approximation

250 To estimate the deflections expected for the bending moments derived here we can use the thin-plate flexure approximations. Many studies of ice shelf bending treat an ice shelf using the plate approximations either with elastic, viscous or viscoelastic rheologies (e.g. Reeh, 1968; MacAyeal and Sergienko, 2013; Olive et al., 2015; Wagner et al, 2016; Banwell et al., 2019; MacAyeal et al., 2021). Vertical deflections of a thin, semi-infinite plate with a moment  $M_T$  applied to the end are given in Turcotte and Schubert (2014) as:

$$255 \quad e^M(x) = e_0^M \exp(-x/\alpha) [\cos(x/\alpha) - \sin(x/\alpha)]$$

and

$$e_0^M = \frac{2M_T}{\rho_w g \alpha^2}$$

(20)



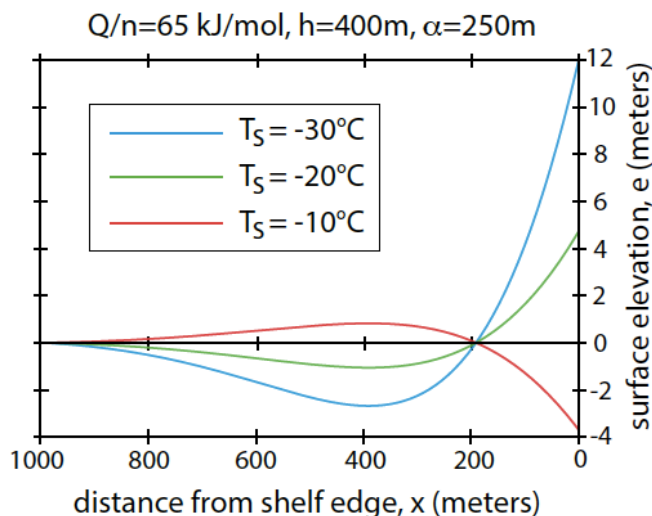
where  $x$  is distance from the shelf edge,  $\alpha$  is the flexure parameter (directly related to the flexural wavelength),  $\rho_w$  is the water  
 260 density, and  $g$  is the acceleration of gravity.

Reeh (1968) and Olive et al. (2016) find that for a viscous or viscoelastic plate with a uniform viscosity  $\eta$  the wavelength of  
 the flexure changes with time as:

$$\alpha(t) \sim \left[ \frac{\eta h^3}{\rho_w g t} \right]^{1/4} . \quad (21)$$

265 where  $t$  is time. This implies that after an early period of rapid change that the flexural wavelength should change slowly with  
 time. Reeh (1968) came to this conclusion and estimated that the long-term flexure parameter can be a bit smaller than the  
 layer thickness. A more through study was done by Olive et al. (2016) who compare fully two-dimensional viscoelastic models  
 of flexure to the thin plate solution and find the best fitting thin plate flexure parameter evolution to match the 2D results. They  
 find that after many Maxwell times (i.e. time  $\gg$  viscosity divided by the elastic shear modulus) that the effective flexure  
 270 parameter is smaller than the layer thickness. Thus, for figures 6 and 7  $\alpha$  is set to 250 m while the ice layer thickness is taken  
 to be 400 m.

Figure 7 shows how the ice surface temperature affects the elevation given by equation 20 for a total moment given by the  
 sum of equations 9 and 19. Figure 6 shows just the predicted deflection of the shelf edge for this model. Given that the internal  
 275 and water-related moment scale with  $h^3$  (via equations 9 and 19) then the combination of this result with equations (20) and  
 (21) implies that for the same rheology, temperature profile and time since calving that the deflection amplitude should scale  
 with  $h^{3/2}$ .





280

**Figure 7: Internal moment model topography versus of distance from a shelf edge predicted for a thin plate subject to an applied moment on the edge. The model ice shelf is taken to be 400 m thick with rheology described in the text with a ratio  $Q/n$  of 65 kJ/mol and the flexure parameter  $\alpha$  is set to 250 m. The surface temperature controls the sign and amplitude of the deflection of the plate edge.**

285

The thin plate approximations can also be used to illustrate the predictions of the bench model. The effect of the load  $V_B$  of a submerged bench on topographic deflections, which (after Wagner et al., 2016) can be written:

$$e^B(x) = e_0^B \exp(-x/\alpha) \cos(x/\alpha)$$

and (22)

290  $e_0^B = \frac{2V_B}{\rho_w g \alpha}$

where  $V_B = w(h - d)(\rho_w - \rho_i)g$  with  $w$  being the width of a bench whose top is just at sea level. Combining this relation for the bench load with equations (21) and (22) suggests that the amplitude of vertical deflections for the bench model should scale linearly with the bench width,  $w$ , but only depend weakly on the ice layer thickness (i.e. bench-driven deflections should scale with  $h^{1/4}$ ). Figure 2 illustrates shows that for the same flexure parameter,  $\alpha$ , the internal moment model produces a much shorter wavelength response than the bench model.

295

#### 4 Discussion and Conclusions

The analysis presented here shows how stresses internal to a floating ice shelf can affect the bending of the shelf edge. It shows that Reeh (1968) was right to be concerned about variations of viscosity through an ice sheet, since those stress determine whether the edge if a shelf bends up or down. For small variations of viscosity across an ice shelf (less than about a factor of about 5) the edge bends down while for larger viscosity variations the edge bends up. Assuming a fairly standard ice flow law and a linear temperature gradient through a shelf, these viscosity variations are controlled by two parameters: the surface temperature,  $T_S$ , and the rheologic parameter ratio of activation volume divided by the power law exponent,  $Q/n$ . The constant  $A$  in the flow-law relation (equation 11) should affect the time over which bending deflections occur, but not the direction or maximum magnitude of those deflections. This “internal moment” model predicts upward bending for cold surface temperatures and large values of the ratio  $Q/n$ .

305

The edge of the Ross Ice Shelf (RIS) offers a good first test of this model for several reasons: it shows rampart and moat structures along most of the front (Becker et al., 2021); it has a low surface temperature (e.g. MacAyeal and Thomas, 1979); and no benches have been reported there. The last point is significant since shelf-edge benches have been seen for several other ice shelves (e.g. Scambos et al., 2005) including recent studies using ICESat 2 lidar (Philipp Arndt, personal comm., 2023).



310 Becker et al. (2021) show strong and systematic variations in the height of upward bending (or in the difference in elevation  
between the moat and rampart,  $\Delta e$ ) and the inferred ice thickness,  $h$ . They find that for  $h = 150$  m the average elevation  
difference,  $\Delta e_M \approx 5$  m, while for  $h = 250$  m they find that  $\Delta e \approx 10$  m. As noted above the internal moment model predicts  
that the elevation difference scales with the ice layer thickness to the power  $3/2$  (i.e. with  $h^{3/2}$ ), and so is consistent with these  
observations. In contrast, the bench model elevations are very weakly dependent on layer thickness (i.e.  $\Delta e_B \sim h^{1/4}$ ) and so do  
315 not explain this trend.

The horizontal offset between ramparts and moats along the RIS front also may be easier to explain with the internal moment  
model than with the bench model. This offset is slightly less than the layer thickness as estimated by Becker et al. (2021). As  
shown in Fig. 2 the lateral scale of deflections for the internal moment model is roughly a factor of two smaller than that of the  
bench model. A detailed comparison of such model predictions must await numerical viscoelastic models since the flexure  
320 parameter is not determined in the present analysis.

The present analysis makes several significant approximations that can be considered in numerical simulations. Such  
simulations are now being done (e.g. Glazer and Buck, 2023) and can treat fully two-dimensional deformation, non-uniform  
vertical temperature gradients, variations of ice density with depth, the time dependence of viscoelastic deformation, among  
325 other factors. Of particular importance will be the calculation of the evolution of the effective flexural wavelength. However,  
the present analysis can guide those model studies since it suggests testable scaling relations including the dependence of  
deflection amplitude on the rheologic parameter  $Q/n$  and the temperature difference across an ice shelf.

Figure 6 shows that for the internal moment model to explain the observed 5-10 meters of upward bending seen along the RIS  
edge requires that the value of the rheologic ratio  $Q/n$  be greater than about 50 kJ/mol. This is at the high end of laboratory,  
330 theoretical and field estimates of this ratio, though uncertainties in estimates of these parameters are large. For example,  
estimates for the flow-law exponent,  $n$ , vary from 1 to 4.5, with higher values corresponding with faster-flowing ice, less  
sliding, and larger grain size (Bons et al., 2018; Zeitz et al., 2020; Millstein et al., 2022, Behn et al., 2021). Likewise,  $Q$  is  
found to vary with temperature (Barnes et al., 1997; Paterson, 1991) with estimated values for cold ice ( $< -10^\circ\text{C}$ ) ranging from  
42 to 85 kJ/mol; and for warmer from 120 to 200 kJ/mol (Zeitz et al., 2020; Greve, 1997; Furst et al., 2011; Lipscomb et al.,  
335 2019; Weertman et al., 1983). Another key result of laboratory studies of ice flow is that at low stress differences ( $\sim < 10^5$  Pa)  
flow is better described by low values of the power-law exponent  $n$  (e.g. Behn et al., 2021). An ice shelf with a cold surface  
temperature the warm lower part of the shelf may only support stress differences on the order of  $10^4$  Pa and so may be in a low  
 $n$  flow regime (as can be seen by combining an estimate of average stress difference via equation 7 with the calculation of  
vertical variations in effective viscosity given by equation 12, and illustrated in Fig. 3).

340 Further numerical and observational tests of the internal moment model may allow new constraints to be placed on these  
rheologic parameters and since models of ice sheet and ice shelf flow depends on these parameters there should be interest in



doing such tests. One important observation is to measure the distribution and size of ice benches since they certainly can affect shelf bending. Key observational tests should also involve comprehensive studies of shelf-edge bending for all the ice shelves of Antarctica and Greenland. Surface temperatures vary for different ice shelves and if the banding characteristics vary systematically with surface temperature this offers hope of giving new constraints on the temperature dependence of ice rheology.

**Code and data availability:** Neither numerical codes nor new data sets were used to prepare this contribution.

**Author contribution:** All work from conceptualization to writing was done by the sole author.

**Competing interests:** The author declares that he has no conflict of interest.

**Acknowledgements:** Thanks to Emily Glazer, Ching-Yao Lai, Till Wagner, Nicolas Sartore, Phillip Arndt, Niall Coffey, Kirsty Tinto and Andrew Hoffman for helpful discussion and comments.

## References

- Banwell, A. F., Willis, I. C., Macdonald, G. J., Goodsell, B. and MacAyeal, D. R.: Direct measurements of ice-shelf flexure caused by surface meltwater ponding and drainage, *Nat. Commun.*, 10, 730, doi:10.1038/s41467-019-08522-5, 2019.
- 355 Barnes, P., Tabor, D., and Walker, J. C. F.: The friction and creep of polycrystalline ice. *Proc. Roy. Soc. London. Ser. A. Math. Phys. Sci.*, 324, 127-155, doi:10.1098/rspa.1971.0132, 1997.
- Becker, M.K., Howard, S. L., Fricker, H. A., Padman, L., Mosbeux, C. and Siegfried, M. R.: Buoyancy-Driven Flexure at the Front of Ross Ice Shelf, Antarctica, Observed with ICESat-2 Laser Altimetry, *Geophys. Res. Lett.*, 48, doi:10.1029/2020GL091207, 2021.
- 360 Behn, M. D., Goldsby, D. L., and Hirth, G.: The role of grain size evolution in the rheology of ice: implications for reconciling laboratory creep data and the Glen flow law, *The Cryosphere*, 15, 4589–4605, doi:10.5194/tc-15-4589-2021, 2021.
- Bons, P. D., Kleiner, T., Llorens, M.-G., Prior, D. J., Sachau, T., Weikusat, I., and Jansen, D.: Greenland ice sheet: Higher nonlinearity of ice flow significantly reduces estimated basal motion. *Geophysical Research Letters*, 45(13), 6542–6548, doi:10.1029/2018GL078356, 2018.
- 365 Buck, W. R.: Accretional curvature of lithosphere at magmatic spreading produces an elastically supported axial high, *J. Geophys. Res.*, 106, 3953-3960, doi:10.1029/2000JB900360, 2001.
- Buck, W. R.: The role of fresh water in driving ice shelf crevassing, rifting and calving, *Earth Planet. Sci. Lett.* 624,118444, doi:10.1016/j.epsl.2023.118444, 2023.
- Christmann, J., Müller, R. and Humbert, A.: On nonlinear strain theory for a viscoelastic material model and its implications for calving of ice shelves, *J. Glaciol.* 65, 212–224, doi:10.1017/jog.2018.107, 2019.
- 370



- Cuffey, K.M. and Paterson, W.S.B.: *The Physics of Glaciers*, Elsevier, Oxford, ISBN 978-0-12-369461-4, 2010.
- DeConto, R.M., Pollard, D., Alley, R.B., Velicogna, I., Gasson, E., Gomez, N., Sadai, S., Condrón, A., Gilford, D.M., Ashe, E.L. and Kopp, R.E.: The Paris Climate Agreement and future sea-level rise from Antarctica, *Nature*, 593, 83-89, doi:10.1038/s41586-021-03427-0, 2021.
- 375 Fürst, J. J., Rybak, O., Goelzer, H., De Smedt, B., de Groen, P., and Huybrechts, P.: Improved convergence and stability properties in a three-dimensional higher-order ice sheet model, *Geoscientific Model Development*, 4, 1133–1149, doi:10.5194/gmd-4-1133-2011, 2011.
- Fürst, J.J., Durand, G., Gillet-Chaulet, F., Tavard, L., Rankl, M., Braun, M. and Gagliardini, O.: The safety band of Antarctic ice shelves, *Nature Climate Change*, 6, 479, doi: 10.1038/nclimate2912, 2016.
- 380 Hooke, R.L.: Flow Law for Polycrystalline Ice in Glaciers: Comparison of Theoretical Predictions, Laboratory Data, and Field Measurements, *Rev. Geophys.*, 19, 664-672 doi: doi:10.1029/RG019i004p00664, 1981.
- Glazer E., Buck R. (2023), Effects of Rheology and Temperature Structure on Viscoelastic Ice Shelf Bending, Abstract (C13C-1140) presented at 2023 AGU Fall Meeting, 2023.
- Glen, J. W.: The creep of polycrystalline ice, *Proc. Roy. Academy Lon. Series A*, 228, 519–538, doi:10.1098/rspa.1955.0066, 385 1955.
- Greve, R.: Application of a polythermal three-dimensional ice sheet model to the Greenland ice sheet: Response to steady-state and transient climate scenarios. *J. Climate*, 10, 901–918, doi:10.1175/1520-0442, 1997.
- Gudmundsson, H.: Ice-shelf buttressing and the stability of marine ice sheets. *The Cryosphere*, 7, 647–655, doi:10.5194/tc-7-647-2013, 2013.
- 390 Lai, C.Y., Kingslake, J., Wearing, M.G., Chen, P.H.C., Gentine, P., Li, H., Spergel, J.J., van Wessem, J.M.: Vulnerability of Antarctica’s ice shelves to meltwater-driven fracture. *Nature* 584, 574–578, doi:10.1038/s41586-020-2627- 8, 2020.
- Lipscomb, W. H., Price, S. F., Hoffman, M. J., Leguy, G. R., Bennett, A. R., Bradley, S. L., Evans, K. J., Fyke, J. G., & Kennedy, J. H.: Description and evaluation of the community ice sheet model (CISM) v2.1. *Geoscientific Model Development*, 12, doi:10.5194/gmd-12-387-2019, 2019.
- 395 MacAyeal, D., Thomas, R.: Ross Ice Shelf temperatures support a history of ice-shelf thickening. *Nature*, 282, 703–705, doi:10.1038/282703a0, 1979.
- MacAyeal, D. and Sergienko, O.: The flexural dynamics of melting ice shelves, *Ann. Glaciol.*, 54, doi: 10.3189/2013AoG63A256 1, 2013.
- MacAyeal D. R., Sergienko O.V., Banwell A. F., Macdonald G. J., Willis I. C., Stevens L.A. Treatment of ice-shelf evolution combining flow and flexure, *J. Glaciol.* 67, 885–902, doi:10.1017/jog.2021.39, 2021.
- 400 Millstein, J. D., Minchew, B. M., and Pegler, S. S.: Ice viscosity is more sensitive to stress than commonly assumed, *Communications Earth & Environment*, 3(1), 1–7. doi:10.1038/s43247-022-00385-x, 2022.
- Mosbeux, C., Wagner, T. J. W., Becker, M. K., & Fricker, H. A.: Viscous and elastic buoyancy stresses as drivers of ice-shelf calving. *J. Glaciol.*, 66, 643–657, doi:10.1017/jog.2020.35, 2020.





- 405 Olive, J.-A., Behn, M. D., Mittelstaedt, E., Ito, G. and Klein, B. Z.: The role of elasticity in simulating long-term tectonic extension, *Geophys. J. Int.*, 205, 728–743, doi:10.1093/gji/ggw044, 2021.
- Parmentier, E.M. and Haxby, W. Thermal stresses in the oceanic lithosphere: evidence from geoid anomalies at fracture zones, *J. Geophys. Res.*, 91, 7193–7204, doi:10.1029/JB091iB07p07193, 1986.
- Paterson, W. S. B.: Why ice-age ice is sometimes “soft”. *Cold Regions Science and Technology*, 20, 75–98, doi:10.1016/0165-410 232X(91)90058-O, 1991.
- Reeh, N.: On the calving of ice from floating glaciers and ice shelves. *J. Glaciol.*, 7, 215–232, doi:10.3189/S00221430000310014, 1968
- Rignot, E., Casassa, G., Gogineni, P., Krabill, W., Rivera, A.U. and Thomas, R.: Accelerated ice discharge from the Antarctic Peninsula following the collapse of Larsen B ice shelf. *Geophys. Res. Lett.*, 31, doi:10.1029/2004GL020697, 2004.
- 415 Scambos, T.A., Bohlander, J.A., Shuman, C.U. and Skvarca, P.: Glacier acceleration and thinning after ice shelf collapse in the Larsen B embayment, Antarctica. *Geophys. Res. Lett.*, 31, doi:10.1029/2004GL020670, 2004.
- Scambos, T., Sergienko, O., Sargent, A., MacAyeal, D. and Fastook, J.: ICESat profiles of tabular iceberg margins and iceberg breakup at low latitudes. *Geophys. Res. Lett.* 32, doi: 10.1029/2005GL023802, 2005.
- Scambos, T., Ross, R., Bauer, R., Yermolin, Y., Skvarca, P., Long, D., et al.: Calving and ice-shelf break-up processes 420 investigated by proxy: Antarctic tabular iceberg evolution during northward drift. *J. Glaciol.*, 54, 579–591, doi:10.3189/002214308786570836, 2008.
- Schoof, C.: Ice sheet grounding line dynamics: Steady states, stability, and hysteresis. *J. Geophys. Res.*, 112, doi:10.1029/2006JF000664, 2007.
- Wagner, T. J. W., Wadhams, P., Bates, R., Elosegui, P., Stern, A., Vella, D., et al.: The “footloose” mechanism: Iceberg decay 425 from hydrostatic stresses. *Geophys. Res. Lett.*, 41, 5522–5529, doi:10.1002/2014GL060832, 2014.
- Wagner, T. J. W., James, T. D., Murray, T., and Vella D.: On the role of buoyant flexure in glacier calving. *Geophys. Res. Lett.* 43, 232–240, doi:10.1002/2015GL067247, 2016.
- Weertman, J.: Deformation of floating ice shelves. *J. Glaciol.*, 3, 38–42, doi:10.3189/S0022143000024710, 1957.
- Weertman, J. (1973). Can a water-filled crevasse reach the bottom surface of a glacier? In *Symposium on the Hydrology of 430 Glaciers*, Cambridge, 7–13, September 1969, International Association of Hydrologic Sciences, 139–145.
- Weertman, J.: Creep deformation of ice, *Ann. Rev. Earth Planet. Sci.*, 11, 215–240, doi:10.1146/annurev.ea.11.050183.001243, 1983.
- Zeitz, M., Levermann, A., and Winkelmann, R.: Sensitivity of ice loss to uncertainty in flow law parameters in an idealized one-dimensional geometry. *The Cryosphere*, 14, 3537–3550, doi:10.5194/tc-14-3537, 2020.